Results in Physics 19 (2020) 103562

Contents lists available at ScienceDirect

Results in Physics

journal homepage: www.elsevier.com/locate/rinp

# Exploring the limits of magnetic field focusing: Simple planar geometries

David Cubero [a], Luca Marmugi [b], Ferruccio Renzoni [b,*]

[a] Departamento de Física Aplicada I, Escuela Politécnica Superior, Universidad de Sevilla, Calle Virgen de África 7, 41011 Sevilla, Spain
[b] Department of Physics and Astronomy, University College London, Gower Street, London WC1E 6BT, United Kingdom

ARTICLE INFO

*Keywords:*
Magnetic field shaping

ABSTRACT

This work explores the possibility to arbitrarily shape in space low-frequency magnetic fields using a recently introduced synthesization technique (Choi et al., 2016). We investigate the ability to focus a magnetic field on a two-dimensional region using magnetic field sources distributed on a parallel plane. In agreement with the recent work, arbitrarily tight focusing is demonstrated possible. However, our results indicate that this comes at the cost of exponentially large power requirements and also leads to exponentially large fields in the region between the source and target planes. This imposes strict limitations on the application of the technique. In addition, we also demonstrate that arbitrary steering of the magnetic field focus within the target region is possible, without any additional cost in terms of power requirement. In exploring the potential for magnetic field synthesis, our findings highlight limits to be considered for practical applications, as well as promising capabilities not identified before.

## 1. Introduction

The low-frequency limit of electromagnetism – rigorously defined as the magnetoquasistatic limit [1] – has been recently attracting a growing interest, due to the wealth of related applications, such as magnetic induction tomography (MIT) [2], contactless power transfer [3,4] and underwater communication [5,6], which involve the use of low-frequency oscillating magnetic fields, typically from a few Hz to a few MHz. However, all these applications ideally require a source which generates a focused low-frequency magnetic field. In fact, in MIT a focused B-field is required to excite eddy currents in the wanted portion of the object, so to increase the in-plane spatial resolution and to facilitate three-dimensional image reconstruction. In contactless power transfer and underwater communication, focused B-fields are essential to retain a non-vanishing strength at a useful distance from the source. The unavailability of suitable sources of focused low-frequency magnetic fields has hampered the progress in the development of the above mentioned applications. Indeed, the standard oscillating magnetic dipole is unfitting for the task, as the B-field vanishes at a short range from the source. Furthermore, the extension of phased-array to the low-frequency limit is unpractical, as it would lead to devices with very large dimensions. Recently a promising approach to fill this gap was introduced by Choi et al. [7,8]. A planar array of adjacent coils – thus not relying on the principles underlying phased arrays – was considered. By appropriately tailoring the currents in the individual coils, it was shown that it is possible to synthesize a focused magnetic field.

This work aims to explore the limits of the technique for the synthesization of focused magnetic fields in two dimensions, for the case of a simple planar geometry of the magnetic sources. In particular, we investigate the number of sources required to obtain a wanted focusing, and the required power, which will turn out to be the most important limiting factor for the technique.

This paper is organized as follows. In Section 2 the problem and the notations are introduced. In Section 3 we present numerical results for magnetic field focusing and steering in one- and two-dimensions, discussing the power requirements in all considered cases, and the limitations imposed on practical applications. The behavior of the field in the direction perpendicular to the target plane is then studied, and the related additional constraints discussed. Conclusions are finally drawn.

## 2. The problem and notations

Our goal is to investigate to what extent it is possible to synthetize a focused low-frequency magnetic field using a set of current-carrying wires, with the current distribution across the wires controlling both the focus size and its position in space.

A target region is introduced, which can be one-dimensional (1D) or two-dimensional (2D). The aim is to focus the magnetic field at an arbitrary point $\mathbf{x} = \mathbf{x_0}$ within this region.

* Corresponding author.
*E-mail addresses:* dcubero@us.es (D. Cubero), l.marmugi@ucl.ac.uk (L. Marmugi), f.renzoni@ucl.ac.uk (F. Renzoni).

https://doi.org/10.1016/j.rinp.2020.103562
Received 25 August 2020; Received in revised form 27 October 2020; Accepted 27 October 2020
Available online 31 October 2020

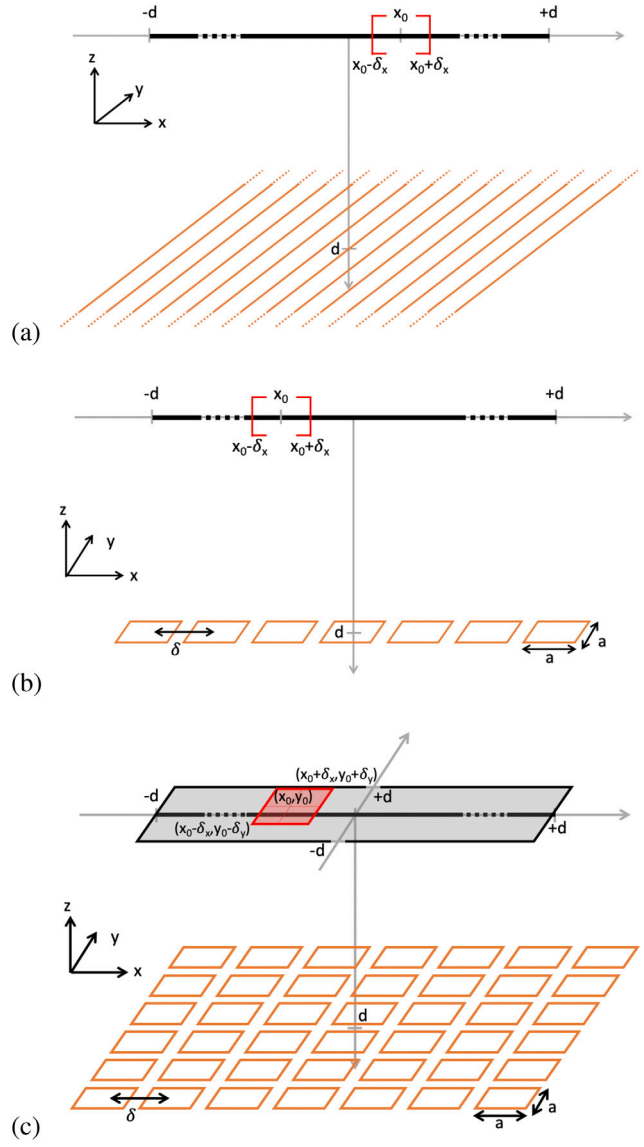


**Fig. 1.** Sketch of the planar arrangements of magnetic field sources considered in the present work. The spot size of the magnetic field at the target region is indicated in red. (For interpretation of the references to color in this figure legend, the reader is referred to the web version of this article.)

Focusing the magnetic field within 1D and 2D target regions has different requirements for the magnetic field sources. Following Refs. [7,8], we consider planar arrangements, which include straight wires and square coils, as sketched in Fig. 1. For 1D target regions, we consider two possible geometries. In the first one, represented in Fig. 1(a), magnetic fields are generated by an array of $N$ infinitely long straight wires carrying electric currents, all parallel to the $y$-axis and crossing the XZ plane at $z = -d$ through equispaced points $x_i$ in the interval between $x = -d$ and $x = d$. In the second one, represented in Fig. 1(b), a 1D array of square coils constitute the source of magnetic fields. The coils, with side length $a$, lie on a plane parallel to the XY plane and intercepting the $z$ axis at $z = -d$. The coils are uniformly distanced one from the other, with their centers spaced of a distance $\delta$. For 2D target regions, the considered magnetic field source, sketched in Fig. 1(c), consists of a 2D array of square coils. As for the 1D case, the coils have side length $a$, lie on a plane parallel to the XY plane and intercept the $z$ axis at $z = -d$. The coils are uniformly distanced one from the other, with their centers spaced of a distance $\delta$.

The extension of the target region is taken to be $2d$ for the 1D case and $4d^2$ for the 2D case. The dimension of the magnetic field "spot size" at the target region (line or plane) will be indicated by $2\delta_x$ for the 1D case and $4\delta_x\delta_y$ for the 2D case.

## 3. Numerical simulations

Our numerical approach to determine the current distribution required for the desired focusing follows the line of Ref. [7]. Details of the procedure are in Appendices A and B. A discrete 1D or 2D grid $\mathbf{x}_i$ (with $i = 1, 2, \ldots, N_\delta$) is superimposed on the target region as applicable, and the currents $I_j$ (with $j = 1, 2, \ldots, N$) in the magnetic field sources (straight wires or coils) are calculated by demanding that the three components of the synthesized field at the discretized points $\mathbf{x}_i$ are all zero, except at $\mathbf{x}_i = \mathbf{x}_0$. The solution for the currents $I_j$ can then be found by matrix inversion, provided that the number $N$ of magnetic field sources (straight wires or coils) is at least three times the number $N_\delta$ of grid points.

We notice that we are considering the quasi-static low-frequency limit of electromagnetism. We thus perform all the calculations as in the static case (dc currents and dc magnetic fields). Results for the low-frequency magnetic fields of interest are then obtained by taking the currents found in the static limit as amplitudes of the ac currents required for the generation of the desired ac magnetic fields.

### 3.1. 1D magnetic field focusing

We first consider the case of 1D magnetic field focusing produced by an array of equally spaced infinitely long wires, with the corresponding set-up shown in Fig. 1(a). The target region is the segment $[-d, d]$ along the $x$-axis ($y = z = 0$). The currents $I_j$ in the wires are calculated by matrix inversion. The field at $x_i = x_0$ is taken as $B_z(x_0, 0, 0) = B_0 = \mu_0 I_0/(2\pi d)$, the field created by a single source at a distance $d$. For this configuration, the resolution is imposed by $\delta_x = 2d/(N_\delta - 1)$. Fig. 2(a, b, c) illustrates 1D magnetic field focusing for the case of straight wires and a line of coils. Here $N = 3N_\delta$ to guarantee that the three components of the magnetic field take the prescribed values at the target points. By appropriately tailoring the current in the different wires (coils), it is possible to synthetize a field which has a maximum around $x_0 = 0$. Furthermore, by increasing by about a factor 2 the number $N$ of sources, it is possible to decrease by the same factor the spot size of the magnetic field.

Magnetic field focusing for the case of a magnetic field source consisting of a line of square coils, as sketched in Fig. 1(b), is illustrated in Fig. 2(d, e, f). Also in this case, it is possible to reduce the magnetic field spot size at the target region by increasing the number $N$ of magnetic sources.

A central issue of the present discussion is the scaling of the current with the focus size. For a given desired spot size, we calculated by matrix inversion the required currents circulating in the different coils, and extracted the maximum value. Fig. 3 shows such a maximum value as a function of the inverse of the spot size, and evidences an exponentially increasing dependence. So, while focusing of the magnetic field down to a desired value is in principle possible, the current required makes focusing below a certain level impractical.

### 3.2. 1D magnetic field steering

We consider here the possibility of steering the magnetic field focus within the target region for a *fixed* configuration of the magnetic field sources, i.e. for fixed number $N$ of the wires/coils and their spatial arrangement. This is very important for magnetic induction tomography, where it would allow to selectively address different areas of the object of interest, thus increasing the resolution.

Steering of the magnetic field focus can be achieved by varying the current distribution among the different wires depending on the

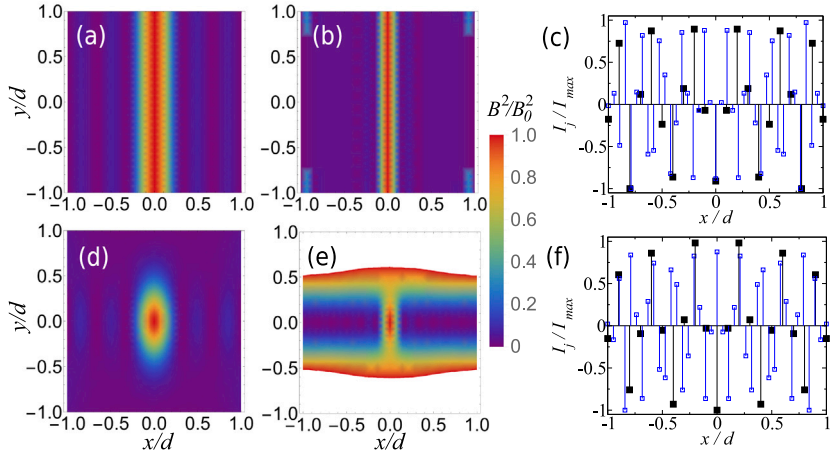


**Fig. 2.** Synthesization of 1D focused magnetic field, for two different configurations of magnetic sources: a set of infinite straight wires along the $y$-axis (a–c) and a set of square coils with length $a = d/2$ (d–f). The target region is along the $x$-axis ($y = 0$ and $z = 0$), separated a distance $d$ from the source plane (at $z = -d$). For all the simulations the number of coils $N$ is three times the number of target points: $N = 3 \times N_\delta$. (a) Infinite straight wires with $\delta_x/d = 1/3$ ($N_\delta = 7$). (b) Infinite straight wires with $\delta_x/d = 1/6$ ($N_\delta = 13$). (c) Current distribution through the different wires to achieve the wanted focusing as in (a) (black large square data set) and (b) (blue small square data set). Each data set is normalized to the maximum current. (d) Square coils with $\delta_x/d = 1/3$. (e) Square coils with $\delta_x/d = 1/6$. The magnetic field magnitude goes beyond the considered scale in the region approximately defined by $|y/d| > 0.5$, and indicated in white in the figure. (f) Current distribution through the different coils to achieve the wanted focusing as in (d) (black large square data set) and (e) (blue small square data set). Each data set is normalized to the maximum current.

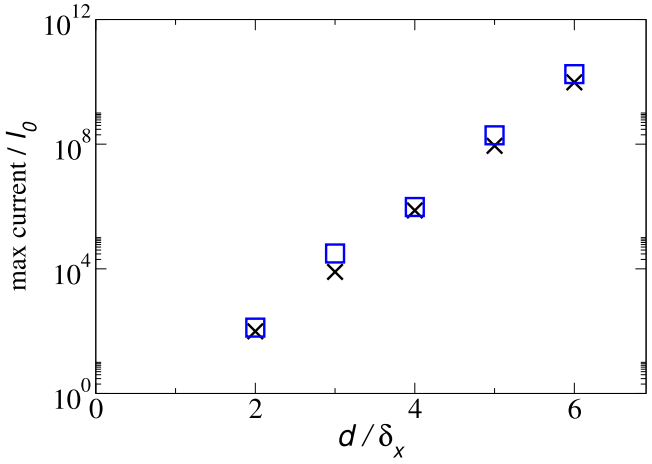


**Fig. 3.** Maximum dimensionless current as a function of the inverse of the resolution in 1D setups. The black crosses are the results for a system using an array of infinite straight lines carrying electric currents, and the blue squares correspond to a linear array of square coils with coil length $a = d/2$. The synthesized field $B_0$ at the focusing point $x_0$ is chosen to coincide with the field created by a single magnetic source at the distance $d$. For all the data points the number of coils $N$ is three times the number of target points: $N = 3 \times N_\delta$.

desired position of the magnetic field focus. This is demonstrated in Fig. 4, where the current distribution among different wires/coils is determined by matrix inversion for different position of the magnetic field focus $x_0$ within the target region. It can be seen that the focus position can be varied, while maintaining the focus size. We notice that there is a distortion whenever the desired focus position approaches the target region boundaries, see Fig. 4. In this case, while the field is forced to equal $B_0$ at $x_0$ by the matrix inversion procedure, it goes above the desired value (white region in the figure) between $x_0$ and the nearest boundary, before decaying to a smaller value. We found that steering with a high degree of control can be achieved in about half of the target region. Obviously, whenever steering has to be achieve on a larger distance, a larger extension of the magnetic field source arrangement has to be considered.

A remarkable and important finding is that steering the magnetic field focus away from the center of the target region does not require a significant increase of the maximum current across the wires/coils (see caption of Fig. 4), at variance with the requirements required for decreasing the focus waist, obtained at the cost of an exponential increase in current.

### 3.3. 2D magnetic field focusing and steering

Magnetic field focusing and steering can be directly generalized to a 2D target region by using the 2D magnetic field source configuration of Fig. 1(c) consisting of an array of square coils of length $a$. Fig. 5 shows numerical results for focusing and steering for the 2D configuration.

The reported results validate for the 2D case what already observed for 1D: by varying the number of coils $N$ and target fixed points $N_\delta$, here taken to be $N = 2^2 N_\delta$, it is possible to decrease the spot size, although this is at the cost of an exponential increase in the current required, as shown in Fig. 6 — like in the 1D case, the field at the focusing point $\mathbf{x}_0$ is required to be that of a single, symmetrically placed coil, here

$$B_0 = \mu_0 I_0 \sqrt{8}/(\sqrt{75}\pi d) \tag{1}$$

(see Appendix A).

For a fixed number of coils, it is possible to steer the focus within the target region without a significant increase in the current required.

As an explicit example, we consider a 2D set-up with $d = 10$ cm, and aim to focus the magnetic field to a spot size of $\delta_x = d/2 = 5$ cm with peak amplitude $B_0 = 0.5 \times 10^{-6}$ T. From the expression for the field a single coil, Eq. (1), which we take as a reference, we derive that the requirement of a field peak amplitude of $B_0 = 0.5 \times 10^{-6}$ T implies a reference current of $I_0 = 0.38$ A. Our results of Fig. 6 show that for $d/\delta_x = 2$ we have $I_{\max}/I_0 = 30$, thus the maximum current required in a single coil is $I_{\max} = 11.4$ A. On the other hand, if we require a 2-fold reduction in the spot size $\delta_x$ for the same distance $d$ and field peak amplitude $B_0$, the current required becomes extremely large, and equal to $I_{max} = 31025$ A.

### 3.4. Behavior outside the target plane

The discussion so far dealt uniquely with the control of the magnetic field within the target plane. This was according to the fact that in this work we do not address the issue of 3D field shaping. Nevertheless, it is interesting to study the field behavior also in the region between the

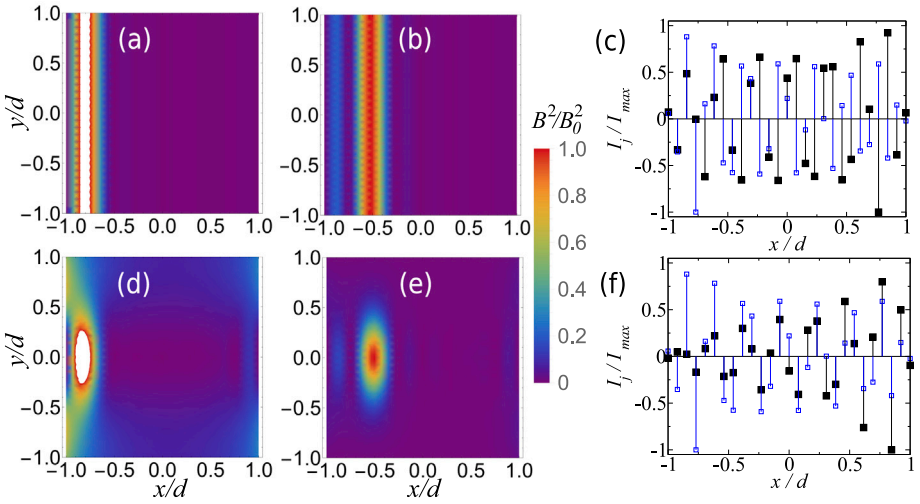


**Fig. 4.** Steering of the 1D magnetic field focus, for the same two configurations of magnetic field sources of Fig. 2. (a) Infinite straight wires with $x_0/d = -0.75$. (b) Infinite straight wires with $x_0/d = -0.5$. (c) Current distribution through the different wires to achieve the wanted steering as in (a) (black large square data set) and (b) (blue small square data set). Each data set is normalized to the maximum current. (d) Square coils with $x_0/d = -0.75$. (e) Square coils with $x_0/d = -0.5$. (f) Current distribution through the different coils to achieve the wanted steering as in (d) (black large square data set) and (e) (blue small square data set). Each data set is normalized to the maximum current. For all calculations $\delta_x/d = 0.25$ ($N_\delta = 9, N = 27$). The white region indicates regions where $B$ goes above the wanted peak value $B_0$, by up to a factor 1.5. The values for $I_{max}$ for the different calculations are as follows. Straight wires: $I_{max}/I_0 = 0.209499 \times 10^6$ for (a), $I_{max}/I_0 = 0.933767 \times 10^6$ for (b), and for comparison $I_{max}/I_0 = 0.373630 \times 10^6$ for the case of $x_0 = 0$. Square coils: $I_{max}/I_0 = 4.43414 \times 10^6$ for (d), $I_{max}/I_0 = 7.17498 \times 10^6$ for (e), and for comparison $I_{max}/I_0 = 2.17439 \times 10^6$ for the case of $x_0 = 0$.

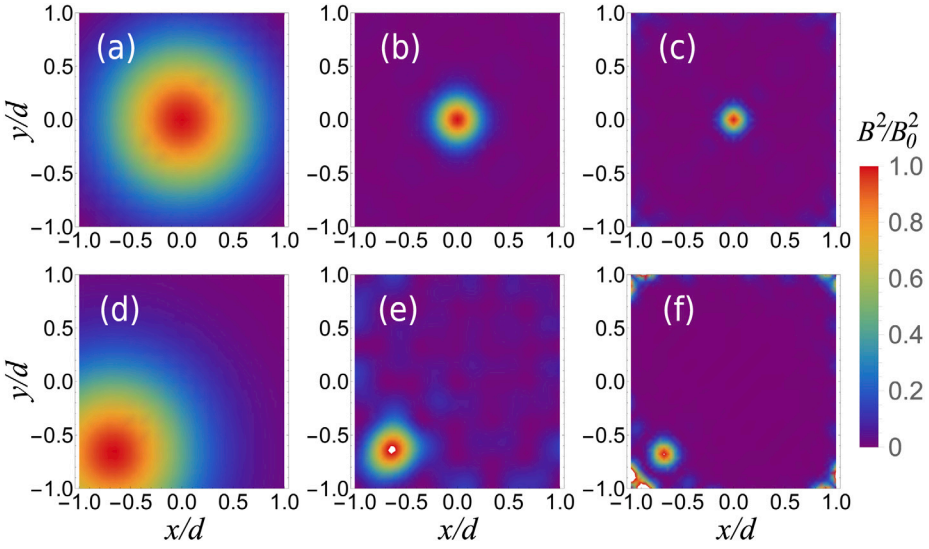


**Fig. 5.** Magnetic field focusing and steering in two dimensions. The first row reports focusing at the center of the target area $\mathbf{x}_0 = (0,0)$ by increasing the number of fixed points from $N_\delta = 7 \times 7$ ($\delta_x/d = 1/3$) in (b) to $N_\delta = 13 \times 13$ ($\delta_x/d = 1/6$) in (c), with (a) being the field for a single coil centered at $\mathbf{x}_0 = (0,0)$, reported for comparison. In all cases $N = 2^2 N_\delta$ and $a = d$. The second row reports focusing at the point $\mathbf{x}_0 = (-2d/3, -2d/3)$. As for the first row, increased focusing is obtained by increasing the number of fixed points from $N_\delta = 7 \times 7$ ($\delta_x/d = 1/3$) in (e) to $N_\delta = 13 \times 13$ ($\delta_x/d = 1/6$) in (f), with (d) the field for a single coil centered at $\mathbf{x}_0 = (-2d/3, -2d/3)$. Thus focusing is demonstrated by moving from the center column to the right one, while steering from the two last panel of the top row to the corresponding ones on the bottom row.

source plane and the target plane, as this may introduce limitations in practical uses of 2D field shaping in its present conception. To this purpose, consider the configuration presented in the panels (b) and (c) of Fig. 5 as case study. The corresponding behavior of the field in the transverse direction, i.e. along $z$ with $x_0 = y_0 = 0$, is represented in Fig. 7. The field turns out to be extremely large in proximity of the sources, and decays rapidly to reach the wanted value at the target plane. For the weaker focusing case, the variation in field amplitude spans five orders of magnitude, while for the more focused configuration a larger variation spanning ten orders of magnitude is observed.

The large values required for the field amplitude between source and target plane should be taken into account for applications which require 2D shaping, as such large fields may not be compatible with the materials between the two planes. Specifically, large fields are compatible with remote power transfer where no conductive material is present in the gap. Similarly, magnetic induction tomography of the surface of nanostructures would not find large fields in the gap region a limiting factor. On the contrary, for biomedical [9,10] and security [11,12] applications of electromagnetic induction imaging, the impact of such large fields would have to be taken into account in designing the imaging systems. Excessively large fields may cause damage to the tissues in between the source and the target tissue, certainly an important limiting factor for biomedical imaging. For through-barrier imaging of relevance to security applications, large fields would lead to large unwanted eddy currents in the material shielding the target object, potentially compromising the imaging approach.

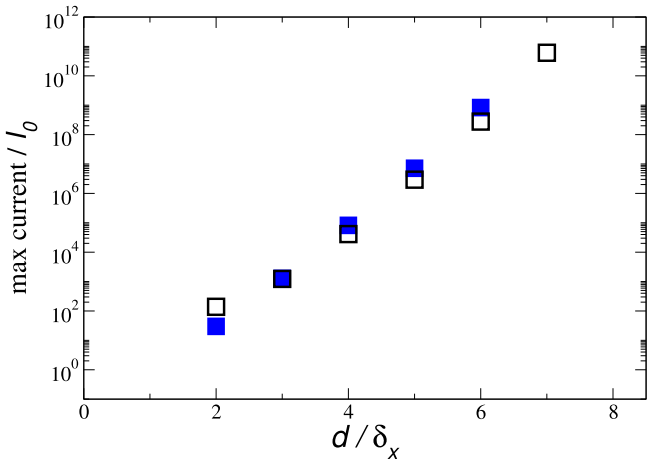


**Fig. 6.** Maximum dimensionless current as a function of the inverse of the resolution in 2D setups. The empty (black) squares are the results for a system using an array of square coils with lengths $a = d$ and the filled (blue) squares correspond to squares coils with $a$ just small enough to avoid overlap between the coils in the source plane.

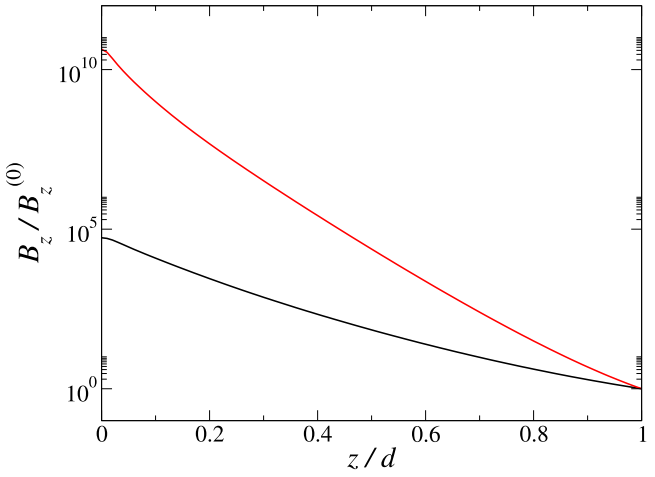


**Fig. 7.** The $z$-component $B_z$ of the magnetic field, normalized by the field $B_z^{(0)}$ created by a single source (square coil), is plotted as a function of $z$ for $\mathbf{x}_0 = (0, 0)$, for the two configurations corresponding to panels (b) and (c) of Fig. 5. The curve in black refers to the configuration of the left panel, the one in red to the right panel. (For interpretation of the references to color in this figure legend, the reader is referred to the web version of this article.)

## 4. Conclusions

Following a recently introduced synthesis technique [7,8], we have investigated the possibility of focusing and steering the magnetic field in 1D and 2D regions by using planar arrays of wires or coils. In agreement with previous work, we found that focusing to any desired level on a target plane is in principle possible by appropriately tailoring the magnetic field source. However, our results also identified important constraints to be taken into account for practical implementations. Firstly, an increase of the focusing level, i.e. a reduction of the magnetic field waist, requires an exponential increase in the current amplitude, which rapidly lead to impracticable power requirements. Secondly, a tight focusing on the target plane produces very large fields in the region between source and target regions – a factor whose impact has to be carefully considered in the application at hand. In addition, we also demonstrated that steering the magnetic focus within the target plane is possible by changing the distribution of currents in the coils, importantly at no additional cost in terms of power requirements.

Despite the limitations highlighted in our work, the synthesis technique considered here is promising for magnetic field beam shaping so to overcome the severe limitations imposed by the standard dipole pattern of a single coil. This paves the way for numerous applications, from efficient transmission of power to high resolution probing and imaging.

### CRediT authorship contribution statement

**David Cubero:** Investigation, Software, Writing - review & editing. **Luca Marmugi:** Methodology, Writing - review & editing. **Ferruccio Renzoni:** Conceptualization, Writing - original draft.

### Declaration of competing interest

The authors declare that they have no known competing financial interests or personal relationships that could have appeared to influence the work reported in this paper.

### Acknowledgment

DC acknowledges financial support from the Ministerio de Ciencia e Innovación of Spain, Grant No. PID2019-105316GB-I00.

### Appendix A. Magnetic field created by a square coil

The magnetic flux density at the position $\mathbf{x} = (x, y, z)$ created by a wire carrying an electric current $I$ is given by the Biot–Savart law [13]

$$\mathbf{B}(\mathbf{x}) = \frac{\mu_0 I}{4\pi} \int \frac{\mathrm{d}\mathbf{l} \times (\mathbf{x} - \mathbf{l})}{|\mathbf{x} - \mathbf{l}|^3}, \tag{A.1}$$

where the integral extends over all wire's positions $\mathbf{l}$. For a straight segment that starts at $\mathbf{l}_1$ and ends at $\mathbf{l}_2$ we have

$$\mathbf{l} = \mathbf{l}_1 + s\mathbf{n}, \tag{A.2}$$

where $0 \le s \le |\mathbf{l}_2 - \mathbf{l}_1|$ and $\mathbf{n} = (\mathbf{l}_2 - \mathbf{l}_1)/|\mathbf{l}_2 - \mathbf{l}_1|$, and thus,

$$\mathbf{B}_{\mathrm{seg}}(\mathbf{x}) = \frac{\mu_0 I}{4\pi} \int_0^{|\mathbf{l}_2 - \mathbf{l}_1|} \mathrm{d}s \frac{\mathbf{n} \times (\mathbf{x} - \mathbf{l}_1)}{|\mathbf{x} - \mathbf{l}_1 - s\mathbf{n}|^3}. \tag{A.3}$$

The integral (A.3) can be straightforwardly evaluated, yielding

$$\mathbf{B}_{\mathrm{seg}}(\mathbf{x}) = \frac{\mu_0 I}{4\pi} \frac{(\mathbf{x} - \mathbf{l}_1) \times (\mathbf{l}_2 - \mathbf{l}_1)}{|(\mathbf{x} - \mathbf{l}_1) \times (\mathbf{l}_2 - \mathbf{l}_1)|^2} \times \left[ \frac{\mathbf{x} - \mathbf{l}_2}{|\mathbf{x} - \mathbf{l}_2|} - \frac{\mathbf{x} - \mathbf{l}_1}{|\mathbf{x} - \mathbf{l}_1|} \right] \cdot (\mathbf{l}_2 - \mathbf{l}_1). \tag{A.4}$$

The magnetic flux density created by a square coil is just the sum of the densities (A.4) created by each of the four segments, with length $|\mathbf{l}_i - \mathbf{l}_{i+1}| = a$, composing the coil.

For a square coil with current $I_0$ and its symmetry axis along the $z$-axis and its center at the origin, the flux density among that axis is given by

$$\mathbf{B}^{(0)}(0, 0, z) = \frac{\mu_0 I_0 \sqrt{8}}{\pi a (1 + 4\frac{z^2}{a^2}) \sqrt{1 + 2\frac{z^2}{a^2}}} \mathbf{e}_z. \tag{A.5}$$

### Appendix B. Calculation of the electric currents

The coils' electric currents are determined by imposing a finite transverse size of the magnetic field at the target region. We use here a similar procedure than the one proposed in [7,8].

The field at the target region is the superposition of the field created by each coil, which, according to Biot–Savart law, is proportional to the coil current $I_0 I_i$, where $I_0$ is a reference current and $I_i$ is a dimensionless variable. Thus,

$$\mathbf{B}(\mathbf{x}) = \sum_{j=1}^{N} I_j \mathbf{B}^{(j)}(\mathbf{x}), \tag{B.1}$$

where $\mathbf{B}^{(j)}(x, y, z)$ is the field created by the coil $j$, divided by its dimensionless current parameter $I_j$.

The $\alpha$-component ($\alpha = x, y$, or $z$) of the generated field $B_\alpha(\mathbf{x})$ is required to satisfy specific values $B^0_\alpha(\mathbf{x}_i)$ at the nodes $i$ of a lattice that maps the entire target region. Thus, from (B.1), the currents $I_j$ are determined by the linear problem

$$\sum_{j=1}^{N} B^{(j)}_\alpha(\mathbf{x}_i) I_j = B^0_\alpha(\mathbf{x}_i), \tag{B.2}$$

where $i = 1, \ldots, N_\delta$, where $B^{(j)}_\alpha(\mathbf{x}_i)$ is the $\alpha$-component of field created by the coil $j$ at the target point $i$.

In (B.2), the number of unknowns ($I_i$) is $N$, the number of coils, and the total number of equations is given by $3N_\delta$, where $N_\delta$ is the number of fixing points, because the three components of the field are fixed at each point in the target region. Thus, we need to consider $N \geq 3N_\delta$.

For convenience, we do not restrict ourselves to $N = 3N_\delta$, but consider the general case $N > 3N_\delta$. Then, there are $N - 3N_\delta$ extra solutions. These extra solutions belong to the nullspace [14] of the corresponding matrix. If we rewrite the linear problem (B.2) as

$$A\chi = \eta, \tag{B.3}$$

where $\chi = (I_1, \ldots, I_N)$ and $\eta$ are vectors of dimension $N$ and $3N_\delta$, respectively, and $A$ is the corresponding matrix of dimensions $(3N_\delta) \times N$, then, we can always find a solution $\chi_0$ that satisfies $A\chi_0 = \eta$, and also $N - 3N_\delta$ linearly independent solutions $\chi_k$ ($k = 1, \ldots, N - 3N_\delta$) which satisfy $A\chi_k = 0$. Any other solution can be written as

$$\chi = \chi_0 + \sum_{k=1}^{N-3N_\delta} a_k \chi_k, \tag{B.4}$$

where $a_k$ are real constants. In view of practical implementations, we are interested in the minimum current solution, that is, the solution that minimizes the quantity $\sum_{j=1}^{N} I_j^2 = \chi \cdot \chi$, which can be found by demanding $\chi$ to be perpendicular to $\chi_k$, i.e.

$$\chi \cdot \chi_k = \sum_{j=1}^{N} I_j I_j^{(k)} = 0. \tag{B.5}$$

Inserting (B.4) into (B.5) yields the following equations for $a_k$

$$\sum_{k=1}^{N-3N_\delta} (\chi_k \cdot \chi_{k'}) a_k = -(\chi_0 \cdot \chi_{k'}). \tag{B.6}$$

The solution $\chi_0$ can be found, and (B.6) solved, using standard linear solving algorithms [15].

## References


[1] Haus HA, Melcher JR. Electromagnetic fields and energy. Englewood Cliffs, NJ: Prentice-Hall; 1989.
[2] Griffiths H. Meas Sci Technol 2001;12:1126.
[3] Ishida H, Kyoden T, Furukawa H. Rev Sci Instrum 2018;89:034706.
[4] Sondhi K, Garraud N, Alabi D, Arnold DP, Garraud A, Avuthu SGR, et al. J Micromech Microeng 2020;29(8):084006.
[5] Gerginov V, da Silva FCS, Howe D. Rev Sci Instrum 2017;88:125005.
[6] Akyildiz IF, Wang P, Sun Z. IEEE Commun Mag 2015;53(11):42–8.
[7] Choi Bo H, Kim Ji H, Cheon Jun P, Rim Chun T. IEEE Magn Lett 2016;7:6501504.
[8] Kim Ji H, Choi Bo H, Kim Hoi R, Rim Chun T. IEEE Trans Ind Electron 2019;66:5558.
[9] Marmugi L, Renzoni F. Sci Rep 2016;6:23962.
[10] Deans C, Marmugi L, Renzoni F. Appl Phys Lett 2020;116(13):133501.
[11] Darrer BJ, Watson JC, Bartlett P, Renzoni F. Sci Rep 2015;5:7944.
[12] Deans C, Marmugi L, Renzoni F. Opt Express 2017;25:17911.
[13] Jackson J. Classical electrodynamics. 3rd ed. New York: John Wiley & Sons; 1998.
[14] Strang G. Linear algebra and its applications. 4th ed. Belmont: Thomson Learning; 2006.
[15] Press W, Teukolsky S, Vetterling W, Flannery BP. Numerical recipes the art of scientific computing. 3rd ed. Cambridge: Cambridge University Press; 2007.